PASCOS 2024

New detector configuration for next-generation accelerator-based long-baseline neutrino experiments

Ankur Nath[a], Cao Van Son[b], Jennifer Thomas[c], Quyen Phan To[b]

[*]Namrup College, Assam, India, ZIP 786623
[b]Institute For Interdisciplinary Research in Science and Education (IFIRSE), ICISE, Vietnam
[c] University College London, London

29TH INTERNATIONAL SYMPOSIUM ON PARTICLES, STRINGS AND COSMOLOGY
organised by
International Centre for Interdisciplinary Science Education (ICISE), Quy Nhon, Vietnam
10th **June, 2024**

Outline

Section 1

Introduction

Section 2

Motivation and Approach

Section 3

Experiment Specifications

Section 4

Results

Section 5

Discussion and Future Scope

Neutrino Oscillations

Talks on July 8 by Prof. J.W.F. Valle and on July 10 by Prof. S.K. Agarwalla, PASCOS 2024

$$P(\nu_\alpha \to \nu_\beta) = \left| \sum_j U^*_{\alpha j} U_{\beta j} e^{-\frac{m_j^2}{2E}L} \right|^2 \quad \text{such that} \quad U_{ij} = \begin{bmatrix} c_{12}c_{13} & s_{12}c_{13} & s_{13}e^{-i\delta_{CP}} \\ -s_{12}c_{23} - c_{12}s_{13}s_{23}e^{i\delta_{CP}} & c_{12}c_{23} - s_{12}s_{13}s_{23}e^{i\delta_{CP}} & c_{13}s_{23} \\ s_{12}s_{23} - c_{12}s_{13}c_{23}e^{i\delta_{CP}} & -c_{12}s_{23} - s_{12}s_{13}c_{23}e^{i\delta_{CP}} & c_{13}c_{23} \end{bmatrix}$$

where, $c_{ij} = \cos\theta_{ij}$, $s_{ij} = \sin\theta_{ij}$ (for $i,j = 1,2,3$ and $\alpha, \beta = e, \mu, \tau$)†.

Table: Global Fit of the oscillation parameters, assuming normal ordering (NO) (νFit 5.3).

Parameter	$\sin^2\theta_{12}$	$\sin^2\theta_{13}(\times 10^{-2})$	$\sin^2\theta_{23}$	$\delta_{CP}(^\circ)$	$\Delta m^2_{21}(10^{-5}\text{eV}^2/c^4)$	$\Delta m^2_{31}(10^{-3}\text{eV}^2/c^4)$
Best fit	0.307	2.201	0.572	197	7.41	2.511

†Prog. Theor. Phys. 28, 870 (1962); Zhur. Eksptl'. i Teoret. Fiz. 34 (1958)

Neutrino Oscillations

Talks on July 8 by Prof. J.W.F. Valle and on July 10 by Prof. S.K. Agarwalla, PASCOS 2024

$$P(\nu_\alpha \to \nu_\beta) = \left| \sum_j U^*_{\alpha j} U_{\beta j} e^{-\frac{m_j^2}{2E}L} \right|^2 \quad \text{such that} \quad U_{ij} = \begin{bmatrix} c_{12}c_{13} & s_{12}c_{13} & s_{13}e^{-i\delta_{CP}} \\ -s_{12}c_{23} - c_{12}s_{13}s_{23}e^{i\delta_{CP}} & c_{12}c_{23} - s_{12}s_{13}s_{23}e^{i\delta_{CP}} & c_{13}s_{23} \\ s_{12}s_{23} - c_{12}s_{13}c_{23}e^{i\delta_{CP}} & -c_{12}s_{23} - s_{12}s_{13}c_{23}e^{i\delta_{CP}} & c_{13}c_{23} \end{bmatrix}$$

where, $c_{ij} = \cos\theta_{ij}$, $s_{ij} = \sin\theta_{ij}$ (for $i,j = 1,2,3$ and $\alpha, \beta = e, \mu, \tau$)†.

Table: Global Fit of the oscillation parameters, assuming normal ordering (NO) (νFit 5.3).

Parameter	$\sin^2\theta_{12}$	$\sin^2\theta_{13}(\times 10^{-2})$	$\sin^2\theta_{23}$	$\delta_{CP}(^\circ)$	$\Delta m^2_{21}(10^{-5}\text{eV}^2/c^4)$	$\Delta m^2_{31}(10^{-3}\text{eV}^2/c^4)$
Best fit	0.307	2.201	0.572	197	7.41	2.511

Unsolved Problems in Neutrino Oscillation Physics

Leptonic CP Violation

- We ask whether $\sin\delta_{CP} = 0$ or not?

Neutrino Mass Hierarchy (MH)

- Whether neutrino MH follows normal ordering (NO) *i.e.* $m_1 < m_2 < m_3$ or inverted ordering (IO) *i.e.* $m_3 < m_1 < m_2$ is still a question.

Mixing angle θ_{23}

- Whether θ_{23} follows maximal mixing *i.e.* 45°, or prefers lower octant (LO, $\theta_{23} < 45^\circ$) to higher octant (HO, $\theta_{23} > 45^\circ$) is of interest to pursue. Talk by Quyen Phan To, July 9, PASCOS 2024

†Prog. Theor. Phys. 28, 870 (1962); Zhur. Eksptl'. i Teoret. Fiz. 34 (1958)

MOTIVATION

$$N_{\nu_\beta} \propto \overbrace{\Phi_\alpha(E)}^{Production} \times \underbrace{\frac{1}{L^2} P_{(\nu_\alpha \to \nu_\beta)}(E, L, \rho; \theta_{12}, \theta_{13}, \theta_{23}, \Delta m^2_{21}, \Delta m^2_{31}, \delta_{CP})}_{Propagation} \times \overbrace{\sigma(E)}^{Interaction} \times \underbrace{\epsilon}_{Detection}$$

Conventional Set-Up

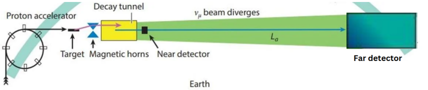

Proposed Set-Up

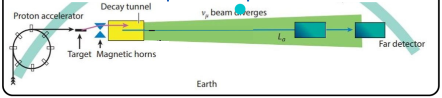

Image Courtesy: Annual Review of Nuclear and Particle Science, 66, (2016)

$$N_{\nu_\beta} \propto \overbrace{\Phi_\alpha(E)}^{Production} \times \underbrace{\frac{1}{L^2} P_{(\nu_\alpha \to \nu_\beta)}(E, L, \rho; \theta_{12}, \theta_{13}, \theta_{23}, \Delta m^2_{21}, \Delta m^2_{31}, \delta_{CP})}_{Propagation} \times \overbrace{\sigma(E)}^{Interaction} \times \underbrace{\epsilon}_{Detection}$$

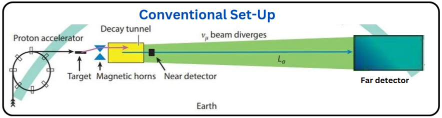

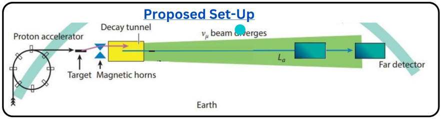

Conventional approach:

- Uses near-site detector (ND) (<1km) to put constraint on the unoscillated neutrino energy spectra.
- Predicts the far-detector (FD) spectra for a specific set of oscillation parameters.
- The use of an ND typically reduces systematics due to (*flux*×*cross-section*) convolution from (10 ∼ 15)% to ∼5% on the event rate.

Image Courtesy: Annual Review of Nuclear and Particle Science, 66, (2016)

$$N_{\nu_\beta} \propto \overbrace{\Phi_\alpha(E)}^{Production} \times \underbrace{\frac{1}{L^2} P_{(\nu_\alpha \to \nu_\beta)}(E, L, \rho; \theta_{12}, \theta_{13}, \theta_{23}, \Delta m^2_{21}, \Delta m^2_{31}, \delta_{CP})}_{Propagation} \times \overbrace{\sigma(E)}^{Interaction} \times \underbrace{\epsilon}_{Detection}$$

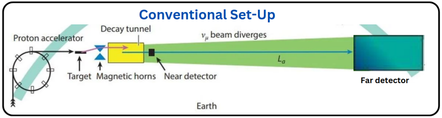

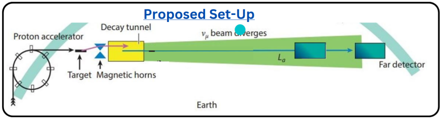

Conventional approach:

- Uses near-site detector (ND) (<1km) to put constraint on the unoscillated neutrino energy spectra.
- Predicts the far-detector (FD) spectra for a specific set of oscillation parameters.
- The use of an ND typically reduces systematics due to (*flux*×*cross-section*) convolution from $(10 \sim 15)\%$ to $\sim 5\%$ on the event rate.

New Set-up:

- **Uses no Near Detector**. Instead a 2nd FD at different baseline of same detector volume as that of the 1st FD is considered.
- The combined fiducial mass is kept intact as that of the single FD as in the conventional approach.
- The role of 2nd detector is not to directly constraint the un-oscillated spectra but to measure the oscillated spectra at a different oscillation length.

Image Courtesy: Annual Review of Nuclear and Particle Science, 66, (2016)

$$N_{\nu_\beta} \propto \overbrace{\Phi_\alpha(E)}^{Production} \times \underbrace{\frac{1}{L^2} P_{(\nu_\alpha \to \nu_\beta)}(E, L, \rho; \theta_{12}, \theta_{13}, \theta_{23}, \Delta m^2_{21}, \Delta m^2_{31}, \delta_{CP})}_{Propagation} \times \overbrace{\sigma(E)}^{Interaction} \times \underbrace{\epsilon}_{Detection}$$

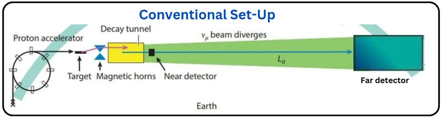

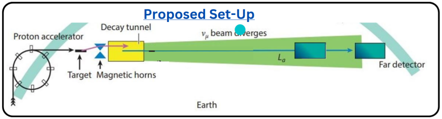

Conventional approach:

- Uses near-site detector (ND) (<1km) to put constraint on the unoscillated neutrino energy spectra.
- Predicts the far-detector (FD) spectra for a specific set of oscillation parameters.
- The use of an ND typically reduces systematics due to (*flux*×*cross-section*) convolution from $(10 \sim 15)\%$ to $\sim 5\%$ on the event rate.

New Set-up:

- **Uses no Near Detector**. Instead a 2nd FD at different baseline of same detector volume as that of the 1st FD is considered.
- The combined fiducial mass is kept intact as that of the single FD as in the conventional approach.
- The role of 2nd detector is not to directly constraint the un-oscillated spectra but to measure the oscillated spectra at a different oscillation length.

With the proposed set-up, relatively large statistics with high power beam (eg. ESSνSB 5MW, T2HK and DUNE $\approx$ MW) can be achieved. Even with large uncertainty in the flux, the correlation in the flux, cross-section and detector response may constrain themselves via the multi-detector data fit.

Image Courtesy: Annual Review of Nuclear and Particle Science, 66, (2016)

Experiments' Specifications: ESSνSB[a]

GLoBES[b] is used to simulate the statistical significance of the experiment.

Baseline:	360km
Beam Power:	5MW
Det. Target:	Water Cherenkov
Det. Volume:	538 ktons
Runtime:	$(5+5)^\dagger$ years

$^\dagger(\nu + \bar{\nu})$ runtime.

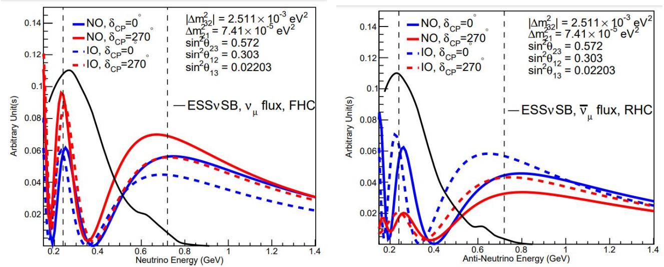

Figure: $P_{\mu e}$ ($P_{\bar{\mu}\bar{e}}$) vs E for NO (*solid*) and IO (dashed) for $\delta_{CP} = 0$ (blue) and 270° (red) values is shown in the *left* (*right*) plot. The fluxes are given by black solid curves.

[a] Eur.Phys.J.ST 231 (2022) 21, 3779-3955. [b] Comput. Phys. Commun. 177 (2007) 432.

N.B. We acknowledge Dr. M. Ghosh of ESSνSB Collab. for sharing the GLoBES-AEDL file.

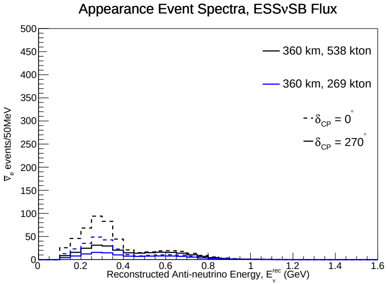

Appearance Event Spectra, ESSνSB Flux
360 km, 538 kton
360 km, 269 kton
δCP = 0°
δCP = 270°
ν̄e events/50MeV
Reconstructed Anti-neutrino Energy, Eν^rec (GeV)

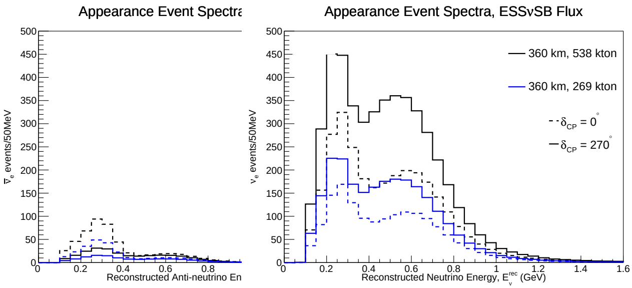

Figure: ν_e ($\bar{\nu}_e$) appearance events as a function of reconstructed neutrino (anti-neutrino) energy for

(a) $\delta_{CP} = 0^\circ$ (dashed)

(b) $\delta_{CP} = 270^\circ$ (solid)

with a

(i) **single far detector** and

(ii) **two far-detectors**

of mass 269 ktons each, is shown in the right (left) plot.

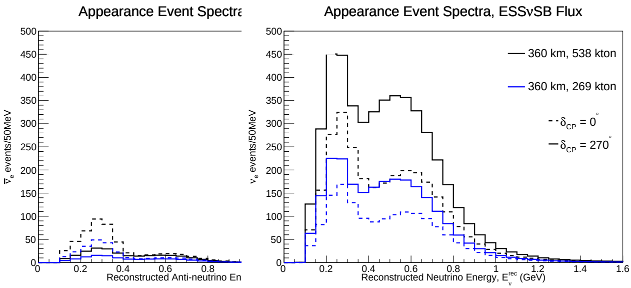

Figure: ν_e ($\bar{\nu}_e$) appearance events as a function of reconstructed neutrino (anti-neutrino) energy for

(a) $\delta_{CP} = 0^\circ$ (dashed)

(b) $\delta_{CP} = 270^\circ$ (solid)

with a

(i) **single far detector** and

(ii) **two far-detectors**

of mass 269 ktons each, is shown in the right (left) plot.

In search of the second baseline...

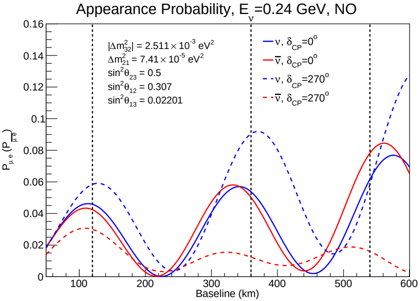

Figure: $P_{\nu_\mu \to \nu_e}$ ($P_{\bar{\nu_\mu} \to \bar{\nu_e}}$) as a function of baseline (in km).

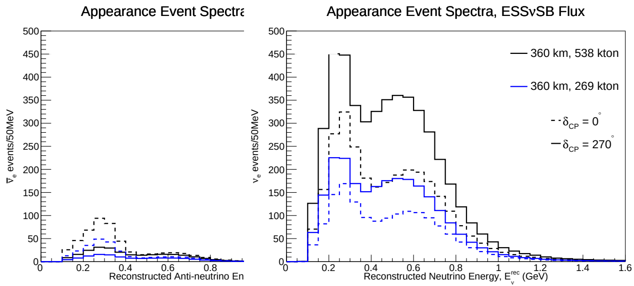

Figure: ν_e ($\bar{\nu}_e$) appearance events as a function of reconstructed neutrino (anti-neutrino) energy for

(a) $\delta_{CP} = 0^\circ$ (dashed)

(b) $\delta_{CP} = 270^\circ$ (solid)

with a

(i) **single far detector** and

(ii) **two far-detectors**

of mass 269 ktons each, is shown in the right (left) plot.

In search of the second baseline...

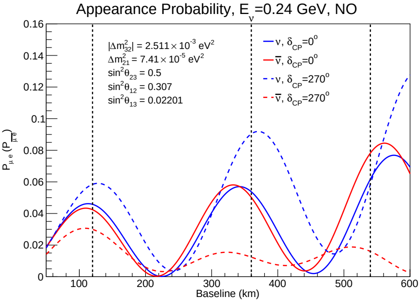

Figure: $P_{\nu_\mu \to \nu_e}$ ($P_{\bar{\nu_\mu} \to \bar{\nu_e}}$) as a function of baseline (in km).

- Oscillation maxima is observed for the case

$$\frac{\Delta m^2_{32} L}{4 E_n} \sim (2n - 1) \times 500 \frac{km}{GeV}$$

where E_n (GeV) is the energy of the nth oscillation peak/dip for a fixed baseline L.

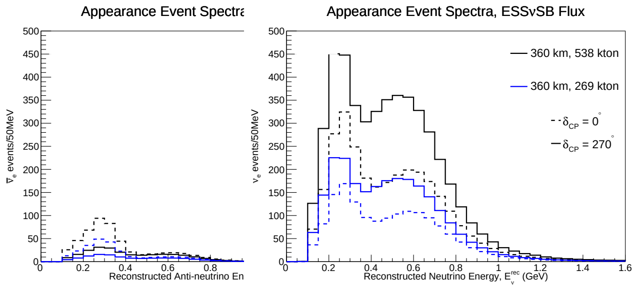

Figure: ν_e ($\bar{\nu}_e$) appearance events as a function of reconstructed neutrino (anti-neutrino) energy for

(a) $\delta_{CP} = 0^\circ$ (dashed)

(b) $\delta_{CP} = 270^\circ$ (solid)

with a

(i) **single far detector** and

(ii) **two far-detectors**

of mass 269 ktons each, is shown in the right (left) plot.

In search of the second baseline...

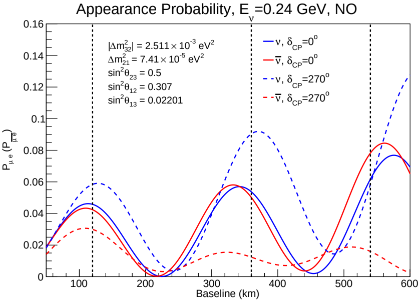

Figure: $P_{\nu_\mu \to \nu_e}$ ($P_{\bar{\nu_\mu} \to \bar{\nu_e}}$) as a function of baseline (in km).

- Oscillation maxima is observed for the case

$$\frac{\Delta m^2_{32} L}{4E_n} \sim (2n-1) \times 500 \frac{km}{GeV}$$

  where E_n (GeV) is the energy of the nth oscillation peak/dip for a fixed baseline L.
- At fixed E=0.24 GeV; 2nd oscillation maxima for L=360km and 1st oscillation maxima for L=120 km are observed.
- Second FD placed at relatively lower baseline means higher statistics.

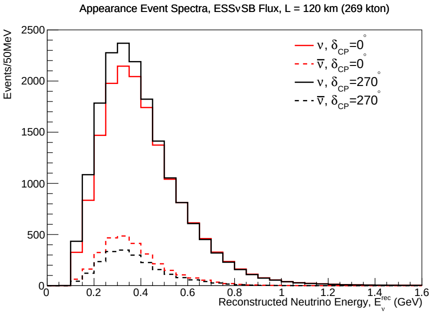
Appearance Event Spectra, ESSνSB Flux, L = 120 km (269 kton)
Events/50MeV
2500
2000
1500
1000
500
0
0
0.2
0.4
0.6
0.8
1
1.2
1.4
1.6
Reconstructed Neutrino Energy, E_{ν}^{rec} (GeV)
ν, δ_{CP}=0°
$\overline{\nu}$, δ_{CP}=0°
ν, δ_{CP}=270°
$\overline{\nu}$, δ_{CP}=270°

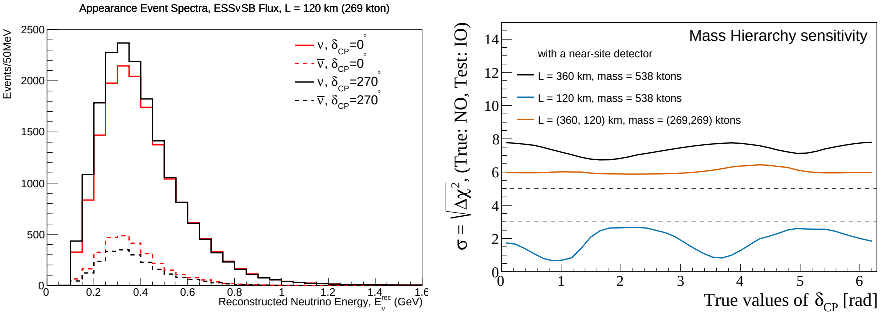

Figure: ***Left:*** Event Spectra for ν_e (solid) and $\bar{\nu}_e$ (dashed) events for $\delta_{CP} = 0$ (red) and 270° (black) for L = 120km, using ESSνSB flux profiles. ***Right:*** Mass Hierarchy sensitivity as a function of true δ_{CP}.

CPV sensitivity plots

The use of far-site detector typically reduce systematics due to flux$\times$cross section convolution from $(10-15)\%$ to $\sim 5\%$ on the event rate.

In these plots,
Systematic errors: 5% represents a set-up of 2FDs ***with*** a near detector.
Systematic errors: 10% represents a set-up of 2FDs ***without*** a near detector.

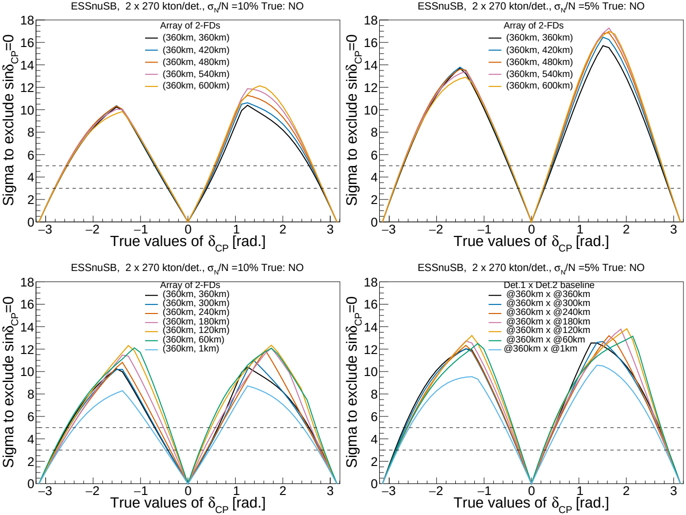

Figure: CPV sensitivity plots.
Top left: Array of 2 FDs with $L2 \geq$ 360km and 10% errors on signal event rates.
Top right: Array of 2 FDs with $L2 \geq$ 360km and 5% errors on signal event rates.
Bottom left: Array of 2 FDs with $L2 \leq$ 360km and 10% errors on signal event rates.
Bottom right: Array of 2 FDs with $L2 \leq$ 360km and 5% errors on signal event rates.

Result

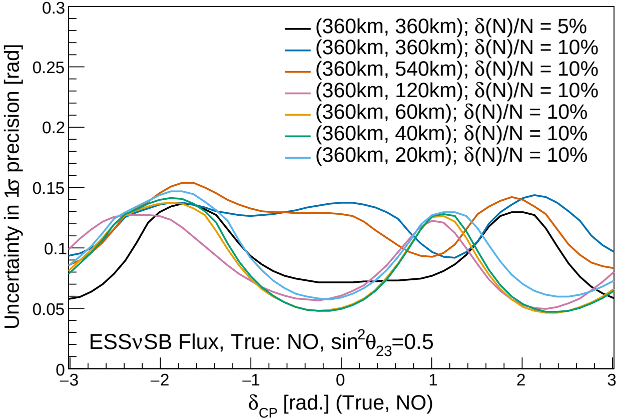

Figure: Uncertanity in 1σ precision measurement of δ_{CP}, considering a single detector FD of fiducial mass of 538kton with a ND **(black solid line)**, compared to that of the cases without a ND with systematic errors of 10% for different FD baseline combinations.

Result

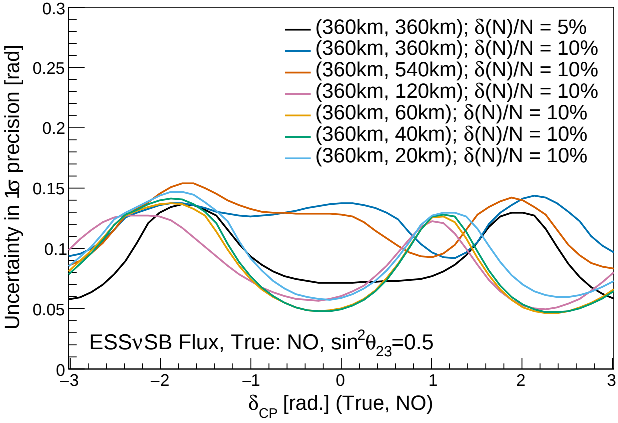

Figure: Uncertainty in 1σ precision measurement of δ_{CP}, considering a single detector FD of fiducial mass of 538kton with a ND **(black solid line)**, compared to that of the cases without a ND with systematic errors of 10% for different FD baseline combinations. Uncertainty in 1σ precision measurement of δ_{CP}, **without a ND** when the 2nd FD is placed at
(i) 540 km (red solid curve), (ii) 120 km (pink), (iii) 60 km (orange), (iv) 40km (green), and (v) 20km (cyan).

Result

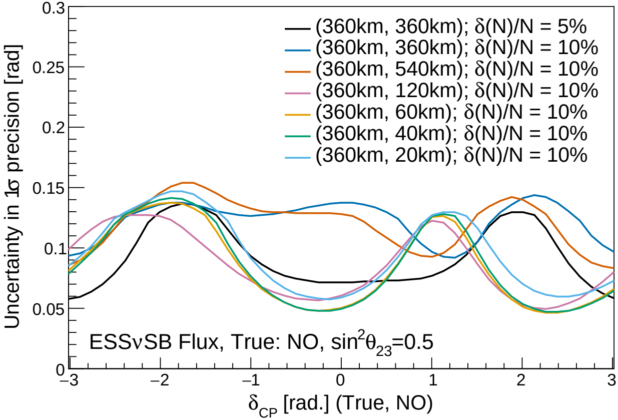

Table: Fraction of true δ_{CP} values for which the proposed set-up **without a ND** gives better 1σ precision of δ_{CP}.

FD Array (*in km*)	Coverage (*in %*)
(360,120)	60
(360, 60)	60
(360, 40)	56
(360, 20)	43.8

Figure: Uncertainty in 1σ precision measurement of δ_{CP}, considering a single detector FD of fiducial mass of 538kton with a ND **(black solid line)**, compared to that of the cases without a ND with systematic errors of 10% for different FD baseline combinations. Uncertainty in 1σ precision measurement of δ_{CP}, **without a ND** when the 2nd FD is placed at
(i) 540 km (red solid curve), (ii) 120 km (pink), (iii) 60 km (orange), (iv) 40km (green), and (v) 20km (cyan).

Result

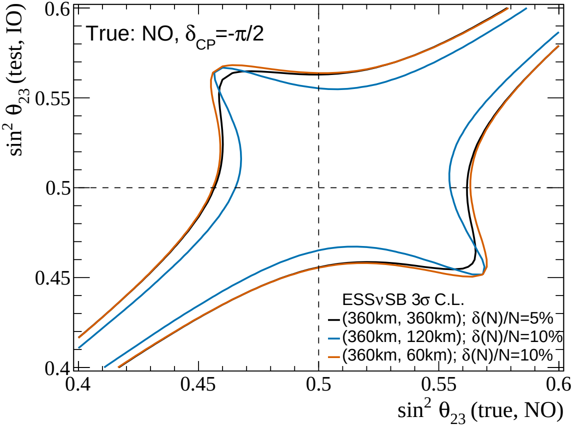

Figure: Allowed region of $\sin^2\theta_{23}$ at a 3σ C.L. for:
(i) ESSνSB with a ND (black solid line)
(ii) 2nd FD placed at 120 km and without a ND (**blue line**).
(iii) 2nd FD placed at 60 km and without a ND (**orange line**).

Discussion & Future Scope

- We investigate the new detector configuration with no near-site detector but multiple far-detectors placed at different baselines, and *it looks promising*.
- 2nd far-detector at 120 km and 60 km (**shorter baseline**) give better precision in the measurement of δ_{CP} for 1σ C.L, for 60% of the true values. Preliminary result shows that θ_{23} can be measured with better precision if the 2nd detector is placed at 120 km.
- Next, we shall quantitatively estmiate the precision on θ_{23} and θ_{13} and $\mathcal{J}$.
    - Precision measurements of δ_{CP}, $\sin^2\theta_{23}$ and $\sin^2 2\theta_{13}$ for discrimination of lepton flavor models.
    - The magnitude of leptonic CPV violation doesn't only depend on δ_{CP}, but is given by the parameterization independent parameter, Jarlskog invariant $\mathcal{J}$:

$$\mathcal{J} = \sin\theta_{12}\cos\theta_{12}\sin\theta_{23}\cos\theta_{23}\sin\theta_{13}\cos^2\theta_{13}\sin\delta_{CP}$$

. Thus, the precision measurement of $\mathcal{J}$ also forms the future scope of this work.

Discussion & Future Scope

- We investigate the new detector configuration with no near-site detector but multiple far-detectors placed at different baselines, and *it looks promising*.
- 2nd far-detector at 120 km and 60 km (**shorter baseline**) give better precision in the measurement of δ_{CP} for 1σ C.L, for 60% of the true values. Preliminary result shows that θ_{23} can be measured with better precision if the 2nd detector is placed at 120 km.
- Next, we shall quantitatively estmiate the precision on θ_{23} and θ_{13} and $\mathcal{J}$.
    - Precision measurements of δ_{CP}, $\sin^2\theta_{23}$ and $\sin^2 2\theta_{13}$ for discrimination of lepton flavor models.
    - The magnitude of leptonic CPV violation doesn't only depend on δ_{CP}, but is given by the parameterization independent parameter, Jarlskog invariant $\mathcal{J}$:

$$\mathcal{J} = \sin\theta_{12}\cos\theta_{12}\sin\theta_{23}\cos\theta_{23}\sin\theta_{13}\cos^2\theta_{13}\sin\delta_{CP}$$

. Thus, the precision measurement of $\mathcal{J}$ also forms the future scope of this work.

OPEN TO QUESTIONS & FEEDBACK...